

Pair correlation function of short-ranged square-well fluids

J. Largo* and J. R. Solana†

Departamento de Física Aplicada, Universidad de Cantabria, E-39005 Santander, Spain

S. B. Yuste‡ and A. Santos§

Departamento de Física, Universidad de Extremadura, E-06071 Badajoz, Spain

(Dated: October 29, 2018)

We have performed extensive Monte Carlo simulations in the canonical (NVT) ensemble of the pair correlation function for square-well fluids with well widths $\lambda - 1$ ranging from 0.1 to 1.0, in units of the diameter σ of the particles. For each one of these widths, several densities ρ and temperatures T in the ranges $0.1 \leq \rho\sigma^3 \leq 0.8$ and $T_c(\lambda) \lesssim T \lesssim 3T_c(\lambda)$, where $T_c(\lambda)$ is the critical temperature, have been considered. The simulation data are used to examine the performance of two analytical theories in predicting the structure of these fluids: the perturbation theory proposed by Tang and Lu [Y. Tang and B. C.-Y. Lu, *J. Chem. Phys.* **100**, 3079, 6665 (1994)] and the non-perturbative model proposed by two of us [S. B. Yuste and A. Santos, *J. Chem. Phys.* **101**, 2355 (1994)]. It is observed that both theories complement each other, as the latter theory works well for short ranges and/or moderate densities, while the former theory does for long ranges and high densities.

I. INTRODUCTION

The study of the thermodynamic and structural properties of square-well (SW) fluids has been the subject of interest for many years because of their simplicity and their resemblance with real fluids with spherically symmetrical potentials, among other reasons. Therefore, at present there are available a considerable number of theories for this kind of fluids. Among them, particularly simple and fruitful are perturbation theories for the thermodynamic properties.^{1,2,3,4,5,6,7,8,9,10} If one is interested in structural properties, one can resort to integral equations theories based on the Ornstein–Zernike equation, for which we have a number of possible choices.^{11,12,13,14,15,16,17,18,19,20,21,22,23,24} The latter group of theories have in general the drawback of being non-analytical, so one has to deal with them by numerical methods. However, in some cases it has been possible to obtain analytical expressions for the structural properties^{25,26,27,28,29,30} inspired, at least indirectly, in integral equation theories.

In parallel with the theoretical developments, a lot of research has been devoted to obtaining the thermodynamic and structural properties of SW fluids by means of computer simulations.^{5,10,14,31,32,33,34,35,36,37,38,39,40,41,42,43,44,45,46,47,48}

Most of that research has focused on SW fluid with intermediate ranges of the potential, because they more closely mimic real simple fluids, whereas relatively little attention has been paid to SW fluids with short ranges. On the other hand, recently there has been a renewal in the interest in short-ranged SW fluids as models of colloidal suspensions^{23,49,50,51,52} and phase separation of protein solutions.⁵³

In the present paper we have carried out Monte Carlo simulations of the pair correlation function or radial distribution function (r.d.f.) $g(r)$ of SW fluids with short, intermediate, and long ranges for temperatures above the critical ones and for a wide range of densities. These

data are used to test the performance of two analytical theories, one perturbative^{27,28} and the other one non-perturbative.²⁹ As we will see, both theories complement each other: the perturbative theory is generally preferable for long ranges, while the non-perturbative theory is better for short ranges.

The plan of the paper is as follows. The two theories are introduced in the next Section, some details being relegated to Appendices A and B. The Monte Carlo method we have employed is succinctly described in Section III. The theoretical results are compared with the simulation data and discussed in Section IV. The main conclusions of the paper are summarized in Section V.

II. ANALYTICAL THEORIES FOR THE PAIR CORRELATION FUNCTION OF SQUARE-WELL FLUIDS

For fluids with a square-well potential of the form

$$u(r) = \begin{cases} \infty & \text{if } r \leq \sigma, \\ -\epsilon & \text{if } \sigma < r \leq \lambda\sigma, \\ 0 & \text{if } r > \lambda\sigma, \end{cases} \quad (1)$$

where λ is the potential range in units of the particle diameter σ and ϵ is the potential depth, several approaches have been devised to derive analytical expressions for the structural properties. In this paper we will focus on two theories, both having in common that analytical expressions for the r.d.f. in Laplace space are provided.

The first one of those theories is due to Tang and Lu (TL),^{27,28} who combined perturbation theory with the mean spherical approximation (MSA) to derive an analytical expression for the first-order r.d.f. $g_1(r)$ in the expansion in power series of the inverse of the reduced temperature $T^* = kT/\epsilon$. Taking for the zeroth-order term $g_0(r)$ the Percus–Yevick (PY) solution,^{54,55} the resulting truncated series for the r.d.f. of the SW fluid is

$$g(x) = g_0(x) + g_1(x) \frac{1}{T^*}, \quad (2)$$

where $x = r/\sigma$. The expressions for the Laplace transforms of $xg_0(x)$ and $xg_1(x)$ are given in Appendix A. The TL theory is expected to be accurate for moderate to large potential widths since the series in powers of $1/T^*$ converges slowly for short-ranged SW potentials.⁵⁶

On the opposite situation, that is, for SW potential with ranges λ close to 1, a procedure has been proposed⁵⁷ to determine the structure of a SW fluid from that of an equivalent fluid of sticky hard spheres, using for the latter Baxter's analytical solution of the PY equation.⁵⁸ To this end, the parameters of the equivalent fluid are determined from the condition that the second virial coefficients of the two fluids must be equal. This approximation provides good results for the structure factor of SW fluids with $\lambda \leq 1.2$, at least for moderate to low densities, but is not appropriate for obtaining the r.d.f., so that it will not be considered in this paper.

As a second theory, we will consider the one developed by Yuste and Santos,²⁹ which provides an alternative analytical expression for short-ranged SW fluids and reduces to Baxter's solution in the sticky hard-sphere limit. We will refer to this theory as the Yuste–Santos (YS) model and it will be presented next with some detail.

The starting point in the YS model is the expression of the Laplace transform $G(t)$ of $xg(x)$ in the form

$$G(t) = t \frac{F(t) e^{-t}}{1 + 12\eta F(t) e^{-t}} = \sum_{n=1}^{\infty} (-12\eta)^{n-1} t [F(t)]^n e^{-nt}, \quad (3)$$

where $\eta = \frac{\pi}{6}\rho\sigma^3$ is the packing fraction, ρ being the number density, and $F(t)$ is an auxiliary function given by^{29,30}

$$F(t) = -\frac{1}{12\eta} \frac{1 + A + K_1 t - (A + K_2 t) e^{-(\lambda-1)t}}{1 + S_1 t + S_2 t^2 + S_3 t^3}. \quad (4)$$

The coefficients K_1 , K_2 , S_1 , S_2 , and S_3 are determined from consistency conditions as functions of η , T^* , λ , and A (see Appendix B). To close the model, the parameter A is further fixed at its zero density value $A = e^{1/T^*} - 1$ for the sake of simplicity.^{29,30} Expression (4) reduces to the exact solutions of the PY equation in the limit of hard spheres ($\lambda \rightarrow 1$ or $T^* \rightarrow \infty$),^{54,55} as well as in the limit of sticky hard spheres ($\lambda \rightarrow 1$ and $T^* \rightarrow 0$ with $T^* \sim -1/\ln(\lambda-1)$).⁵⁸ Therefore, the approximation (4) can be considered as an extension to finite widths of Baxter's solution of the PY equation for sticky hard spheres.

The inverse Laplace transform of Eq. (3) allows us to obtain the r.d.f. in the form

$$g(x) = x^{-1} \sum_{n=1}^{\infty} (-12\eta)^{n-1} f_n(x-n) \Theta(x-n), \quad (5)$$

where the function $f_n(x)$ is the inverse Laplace transform of $t[F(t)]^n$ and $\Theta(x)$ is Heaviside's step function. Note that, to determine the r.d.f. for $x < n+1$ only the first n terms in the summation (5) are needed. In the analysis of Section IV, we will consider reduced distances $x < 3$, so that only the functions f_1 and f_2 will be needed. They are given in Appendix B.

III. MONTE CARLO SIMULATIONS

We have performed NVT Monte Carlo (MC) simulations of the r.d.f. of SW fluids with ranges $\lambda = 1.05$ and $\lambda = 1.1$ – 2.0 (with a step $\Delta\lambda = 0.1$) for (reduced) number densities $\rho^* \equiv \rho\sigma^3 = 0.1$ – 0.8 (with a step $\Delta\rho^* = 0.1$) and several temperatures in the supercritical region. To this end, a system consisting of 512 particles was considered. The particles were initially placed in a regular configuration in a cubic volume with periodic boundary conditions, with fixed temperature and density. After equilibration, the r.d.f. was determined from measurements performed over 5×10^4 cycles, each of them consisting of an attempted move per particle. Results for the contact values $g(1^+)$ of the r.d.f., as well as for their values $g(\lambda^-)$ and $g(\lambda^+)$ at both sides of the potential range, were obtained from extrapolation and are reported in Table I.⁵⁹ From these values, the compressibility factor $Z = pV/NkT$ can be obtained from the virial theorem for the SW fluid as

$$Z = 1 + \frac{2}{3}\pi\rho^* \{g(1^+) - \lambda^3 [g(\lambda^-) - g(\lambda^+)]\}. \quad (6)$$

Values of Z thus obtained were reported elsewhere,⁴⁸ except for the range $\lambda = 1.05$.

TABLE I: MC simulation data of $g(1^+)$, $g(\lambda^-)$, and $g(\lambda^+)$.

ρ^*	0.10	0.20	0.30	0.40	0.50	0.60	0.70	0.80	0.90
$\lambda = 1.05$									
$T^* = 0.5$									
$g(1^+)$	7.304	7.323	7.343	7.501	7.662	7.771	8.081	8.524	9.078
$g(\lambda^-)$	7.278	7.250	7.210	7.317	7.374	7.400	7.587	7.832	8.154
$g(\lambda^+)$	0.987	0.980	0.979	0.988	0.999	0.999	1.030	1.059	1.105
$T^* = 0.7$									
$g(1^+)$	4.382	4.609	4.899	5.194	5.557	6.009	6.505	7.223	8.065
$g(\lambda^-)$	4.321	4.562	4.765	4.986	5.237	5.539	5.842	6.263	6.657
$g(\lambda^+)$	1.034	1.081	1.142	1.195	1.257	1.325	1.401	1.504	1.595
$T^* = 1.0$									
$g(1^+)$	2.964	3.215	3.552	3.891	4.336	4.833	5.457	6.258	7.245
$g(\lambda^-)$	2.923	3.153	3.417	3.679	4.009	4.356	4.759	5.197	5.666
$g(\lambda^+)$	1.071	1.162	1.255	1.355	1.477	1.599	1.746	1.912	2.085
$\lambda = 1.10$									
$T^* = 0.5$									
$g(1^+)$	7.254	7.080	6.628	6.461	6.088	5.836	5.667	5.620	5.810
$g(\lambda^-)$	7.179	6.919	6.463	6.219	5.816	5.519	5.307	5.180	5.162
$g(\lambda^+)$	0.973	0.931	0.875	0.840	0.787	0.746	0.718	0.701	0.698
$T^* = 0.7$									
$g(1^+)$	4.135	4.153	4.174	4.222	4.334	4.529	4.746	5.064	5.604
$g(\lambda^-)$	4.097	4.064	4.028	4.007	4.028	4.096	4.135	4.202	4.284
$g(\lambda^+)$	0.979	0.970	0.964	0.961	0.966	0.980	0.988	1.007	1.027
$T^* = 1.0$									

TABLE I: Continued.

ρ^*	0.10	0.20	0.30	0.40	0.50	0.60	0.70	0.80	0.90
$g(1^+)$	2.829	2.963	3.134	3.320	3.565	3.868	4.263	4.778	5.481
$g(\lambda^-)$	2.790	2.862	2.974	3.068	3.186	3.316	3.463	3.589	3.713
$g(\lambda^+)$	1.026	1.058	1.090	1.128	1.172	1.220	1.273	1.316	1.362
$\lambda = 1.20$									
$T^* = 0.7$									
$g(1^+)$	4.126	4.007	3.805	3.562	3.449	3.297	3.281	3.457	3.921
$g(\lambda^-)$	4.030	3.822	3.555	3.299	3.122	2.924	2.810	2.738	2.612
$g(\lambda^+)$	0.968	0.914	0.850	0.792	0.748	0.700	0.675	0.657	0.628
$T^* = 1.0$									
$g(1^+)$	2.671	2.662	2.666	2.721	2.799	2.941	3.173	3.564	4.232
$g(\lambda^-)$	2.628	2.551	2.489	2.447	2.415	2.388	2.372	2.326	2.208
$g(\lambda^+)$	0.968	0.942	0.918	0.900	0.888	0.880	0.871	0.856	0.812
$T^* = 1.5$									
$g(1^+)$	2.016	2.092	2.212	2.355	2.541	2.807	3.168	3.692	4.513
$g(\lambda^-)$	1.956	1.973	1.991	2.019	2.042	2.059	2.063	2.028	1.917
$g(\lambda^+)$	1.004	1.012	1.021	1.036	1.050	1.057	1.059	1.039	0.982
$\lambda = 1.30$									
$T^* = 1.0$									
$g(1^+)$	2.660	2.592	2.485	2.435	2.414	2.492	2.703	3.136	4.051
$g(\lambda^-)$	2.584	2.433	2.259	2.138	2.033	1.948	1.865	1.737	1.487
$g(\lambda^+)$	0.952	0.896	0.830	0.786	0.748	0.716	0.685	0.639	0.547
$T^* = 1.5$									
$g(1^+)$	1.957	1.982	2.033	2.105	2.245	2.476	2.829	3.409	4.390
$g(\lambda^-)$	1.872	1.834	1.792	1.754	1.720	1.680	1.611	1.486	1.272
$g(\lambda^+)$	0.966	0.940	0.919	0.901	0.883	0.863	0.828	0.763	0.652
$T^* = 2.0$									
$g(1^+)$	1.711	1.770	1.880	2.012	2.214	2.497	2.916	3.558	4.537
$g(\lambda^-)$	1.622	1.618	1.611	1.606	1.582	1.555	1.489	1.368	1.176
$g(\lambda^+)$	0.990	0.981	0.979	0.972	0.962	0.944	0.903	0.829	0.710
$\lambda = 1.40$									
$T^* = 1.0$									
$g(1^+)$	2.899	2.840	2.640	2.398	2.246	2.245	2.515	3.162	4.351
$g(\lambda^-)$	2.679	2.488	2.227	1.966	1.783	1.669	1.544	1.332	1.055
$g(\lambda^+)$	0.986	0.918	0.819	0.725	0.657	0.616	0.568	0.491	0.389
$T^* = 1.5$									
$g(1^+)$	1.928	1.916	1.917	1.977	2.075	2.307	2.716	3.442	4.571
$g(\lambda^-)$	1.836	1.742	1.656	1.583	1.518	1.441	1.328	1.149	0.932
$g(\lambda^+)$	0.945	0.894	0.849	0.811	0.778	0.740	0.681	0.589	0.478
$T^* = 2.0$									
$g(1^+)$	1.665	1.705	1.788	1.889	2.070	2.362	2.834	3.584	4.719
$g(\lambda^-)$	1.588	1.533	1.489	1.444	1.400	1.331	1.227	1.067	0.866
$g(\lambda^+)$	0.960	0.929	0.905	0.877	0.852	0.807	0.743	0.646	0.525
$\lambda = 1.50$									
$T^* = 1.5$									
$g(1^+)$	1.952	1.909	1.884	1.888	1.989	2.263	2.783	3.640	4.962
$g(\lambda^-)$	1.832	1.695	1.570	1.464	1.382	1.281	1.150	0.993	0.850
$g(\lambda^+)$	0.941	0.870	0.804	0.751	0.709	0.659	0.590	0.510	0.437
$T^* = 2.0$									
$g(1^+)$	1.661	1.660	1.720	1.820	2.006	2.336	2.880	3.740	5.013
$g(\lambda^-)$	1.563	1.478	1.403	1.338	1.274	1.185	1.063	0.922	0.790
$g(\lambda^+)$	0.945	0.894	0.851	0.814	0.771	0.719	0.646	0.558	0.480
$T^* = 3.0$									
$g(1^+)$	1.444	1.521	1.628	1.795	2.046	2.424	2.998	3.825	5.025
$g(\lambda^-)$	1.351	1.313	1.268	1.230	1.171	1.090	0.982	0.857	0.728
$g(\lambda^+)$	0.968	0.938	0.909	0.878	0.839	0.781	0.704	0.614	0.521
$\lambda = 1.60$									
$T^* = 1.5$									
$g(1^+)$	2.064	2.026	1.949	1.894	2.004	2.339	3.002	3.996	5.382
$g(\lambda^-)$	1.869	1.696	1.528	1.387	1.293	1.200	1.099	1.015	0.956
$g(\lambda^+)$	0.958	0.872	0.784	0.713	0.665	0.618	0.565	0.521	0.491
$T^* = 2.0$									
$g(1^+)$	1.655	1.673	1.702	1.795	2.007	2.393	3.037	3.985	5.313

TABLE I: Continued.

ρ^*	0.10	0.20	0.30	0.40	0.50	0.60	0.70	0.80	0.90
$g(\lambda^-)$	1.542	1.446	1.350	1.271	1.199	1.110	1.015	0.932	0.872
$g(\lambda^+)$	0.940	0.873	0.819	0.770	0.726	0.673	0.615	0.564	0.530
$T^* = 3.0$									
$g(1^+)$	1.439	1.498	1.602	1.762	2.040	2.463	3.087	3.987	5.258
$g(\lambda^-)$	1.329	1.269	1.218	1.165	1.100	1.021	0.933	0.850	0.792
$g(\lambda^+)$	0.953	0.912	0.873	0.834	0.788	0.732	0.669	0.611	0.567
$\lambda = 1.70$									
$T^* = 2.0$									
$g(1^+)$	1.716	1.714	1.752	1.833	2.077	2.538	3.250	4.253	5.611
$g(\lambda^-)$	1.551	1.432	1.322	1.237	1.165	1.101	1.045	1.017	1.022
$g(\lambda^+)$	0.944	0.870	0.802	0.749	0.706	0.668	0.634	0.617	0.619
$T^* = 3.0$									
$g(1^+)$	1.430	1.494	1.598	1.779	2.083	2.549	3.222	4.160	5.454
$g(\lambda^-)$	1.318	1.251	1.184	1.131	1.069	1.009	0.956	0.928	0.933
$g(\lambda^+)$	0.949	0.893	0.849	0.810	0.766	0.725	0.685	0.664	0.667
$T^* = 5.0$									
$g(1^+)$	1.299	1.403	1.554	1.779	2.114	2.567	3.220	4.108	5.351
$g(\lambda^-)$	1.177	1.139	1.097	1.052	1.000	0.941	0.893	0.860	0.867
$g(\lambda^+)$	0.964	0.934	0.898	0.861	0.818	0.771	0.731	0.703	0.709
$\lambda = 1.80$									
$T^* = 2.0$									
$g(1^+)$	1.839	1.916	1.880	1.932	2.199	2.708	3.487	4.508	5.886
$g(\lambda^-)$	1.599	1.468	1.326	1.233	1.175	1.144	1.141	1.183	1.312
$g(\lambda^+)$	0.974	0.892	0.805	0.745	0.714	0.694	0.693	0.716	0.793
$T^* = 3.0$									
$g(1^+)$	1.449	1.522	1.629	1.828	2.162	2.670	3.392	4.325	5.627
$g(\lambda^-)$	1.320	1.238	1.175	1.124	1.079	1.046	1.043	1.079	1.195
$g(\lambda^+)$	0.942	0.888	0.840	0.803	0.773	0.751	0.747	0.772	0.853
$T^* = 5.0$									
$g(1^+)$	1.297	1.411	1.562	1.809	2.152	2.646	3.318	4.214	5.465
$g(\lambda^-)$	1.169	1.126	1.085	1.042	1.005	0.978	0.970	1.003	1.107
$g(\lambda^+)$	0.956	0.921	0.886	0.854	0.822	0.800	0.794	0.821	0.906
$\lambda = 1.90$									
$T^* = 3.0$									
$g(1^+)$	1.492	1.570	1.692	1.908	2.274	2.815	3.533	4.450	5.534
$g(\lambda^-)$	1.323	1.247	1.182	1.142	1.123	1.132	1.174	1.265	1.403
$g(\lambda^+)$	0.949	0.895	0.848	0.818	0.805	0.811	0.841	0.908	1.008
$T^* = 5.0$									
$g(1^+)$	1.309	1.416	1.587	1.847	2.222	2.733	3.404	4.268	5.353
$g(\lambda^-)$	1.170	1.123	1.087	1.058	1.044	1.049	1.089	1.174	1.305
$g(\lambda^+)$	0.958	0.920	0.889	0.867	0.855	0.859	0.891	0.961	1.072
$\lambda = 2.00$									
$T^* = 3.0$									
$g(1^+)$	1.564	1.699	1.824	2.032	2.424	2.973	3.669	4.493	5.499
$g(\lambda^-)$	1.346	1.282	1.217	1.192	1.199	1.245	1.322	1.425	1.528
$g(\lambda^+)$	0.968	0.918	0.873	0.853	0.861	0.892	0.949	1.024	1.100
$T^* = 5.0$									
$g(1^+)$	1.325	1.450	1.633	1.907	2.300	2.814	3.471	4.304	5.354
$g(\lambda^-)$	1.178	1.131	1.105	1.098	1.109	1.152	1.225	1.326	1.428
$g(\lambda^+)$	0.960	0.926	0.905	0.899	0.910	0.944	1.005	1.089	1.175

IV. RESULTS AND DISCUSSION

The objective is to determine the limits of applicability of the TL and YS theories. We are mainly interested in the domain of *moderate* temperatures. By that we mean temperatures within the range $T_c^*(\lambda) \lesssim T^* \lesssim 3T_c^*(\lambda)$, where $T_c^*(\lambda)$ denotes the critical temperature of

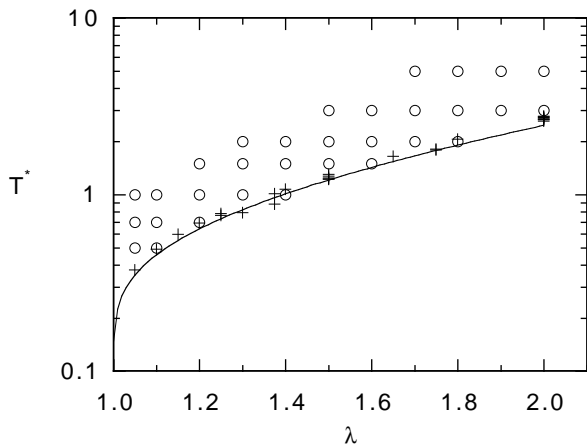


FIG. 1: The open circles represent the values of the reduced temperature T^* we have considered for each value of the range λ . The crosses are simulation data for the critical temperature $T_c^*(\lambda)$ (see Ref. 24) and the solid line is the theoretical estimate (7). Note the logarithmic scale of the vertical axis.

the SW fluid with range λ . This critical temperature has been measured in computer simulations for several ranges.^{39,40,41,42,43,44,53} Table I of Ref. 24 gives a rather extensive compilation of data. A simple analytical estimate for $T_c^*(\lambda)$ was derived in Ref. 30:

$$T_c^*(\lambda) = \frac{1}{\ln \left[1 + \frac{3+\lambda+2\sqrt{2\lambda}}{\lambda(\lambda-1)(9-2\lambda+\lambda^2)} \right]}. \quad (7)$$

Figure 1 is a T^* - λ plot where the open circles represent the three temperatures (two in the cases $\lambda = 1.9$ and $\lambda = 2$) we have considered in the simulations for each value of λ . The simulation data of $T_c^*(\lambda)$,²⁴ as well as the theoretical estimate (7) are also shown. For each value of λ we have typically considered three temperatures: $T_1^* \gtrsim T_c^*$, $T_2^* \approx 1.5T_1^*$, and $T_3^* \approx 2T_1^*$, so that $T_3^* \gtrsim 3T_c^*(\lambda)$.

Before comparing the simulation data of the full r.d.f. with the theoretical predictions, it is worth focusing on the contact value $g(1^+)$. Figures 2 and 3 show $g(1^+)$ as a function of the reduced density for the temperatures represented in Fig. 1, as obtained from our MC simulations, as well as from the TL and YS theories [cf. Eqs. (A6), (A9), and (B5)]. We observe that for $\lambda = 1.05$ and $\lambda = 1.1$ the non-perturbative YS model presents a very good agreement with the simulation data for the three temperatures considered, whereas the TL perturbation theory is rather poor, especially for low temperatures. For $\lambda \geq 1.2$, however, the YS model behaves well for small and moderate densities but starts to fail in the high-density domain, especially for the lowest temperature, the failure being more dramatic as the well width increases. Interestingly, the TL theory becomes more accurate precisely in that high-density region where the YS model is less reliable. Thus, for a given range λ , there exists a certain threshold density $\rho_0^*(\lambda)$ such that the YS model is accurate for $\rho^* \lesssim \rho_0^*(\lambda)$ and inaccurate

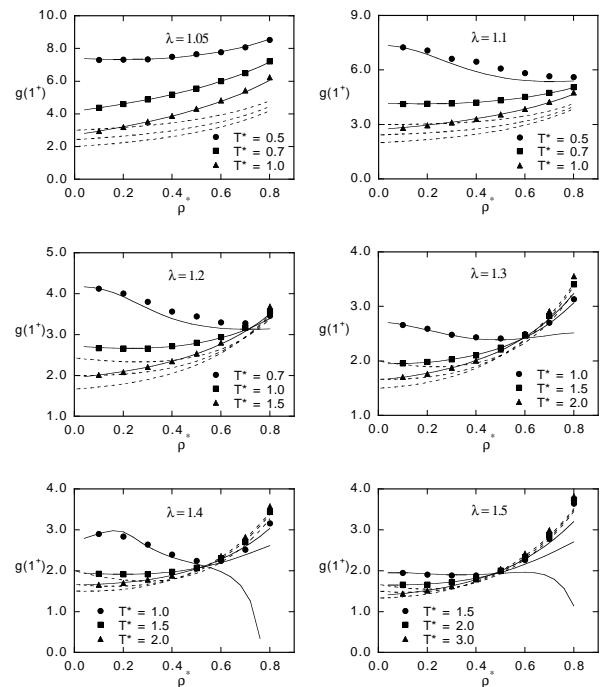


FIG. 2: Comparison of the contact values $g(1^+)$ of the r.d.f. obtained from the TL (dashed lines) and YS (solid lines) theories with Monte Carlo data as functions of the reduced density ρ^* for different temperatures and well widths $\lambda = 1.05$ – 1.5 .

for $\rho^* \gtrsim \rho_0^*(\lambda)$, while the opposite situation occurs in the case of the TL theory. Of course, this qualitative description applies for the range of “moderate” temperatures defined above, since the results obtained from both theories tend to coincide as the temperature increases.

According to Figs. 2 and 3, the location of $\rho_0^*(\lambda)$ roughly coincides with the region where either the isotherms cross (for $\lambda \leq 1.7$) or have the least separation (for $1.8 \leq \lambda \leq 2.0$). This means that the simulation data of $g(1^+)$ in the region $\rho^* \approx \rho_0^*(\lambda)$ are practically insensitive to the temperature, so they are close to its hard-sphere value $g_0(1^+)$. For larger densities, $\rho^* \gtrsim \rho_0^*(\lambda)$, the simulation data show that the influence of temperature is small and hence the TL perturbation theory becomes accurate in that domain. On the other hand, for $\rho^* \lesssim \rho_0^*(\lambda)$ the MC values of $g(1^+)$ are strongly sensitive to temperature, as expected from the fact that at zero density $g(1^+) = e^{1/T^*}$, while perturbation theories give $g(1^+) = 1 + 1/T^*$. The strong deviation of the non-perturbative YS theory from the MC data in the density region $\rho^* \gtrsim \rho_0^*(\lambda)$, especially for $\lambda \geq 1.4$, is in part due to the fact that in the YS model the parameter A in Eq. (4) is assumed to be independent of density and so it is assigned its zero-density value $A = e^{1/T^*} - 1$. A better agreement is expected if A is allowed to depend on density, but this would imply either to impose an extra consistency condition (for instance, continuity of the first derivative of the cavity function) or to apply an empirical fit, what is outside the original spirit of the YS

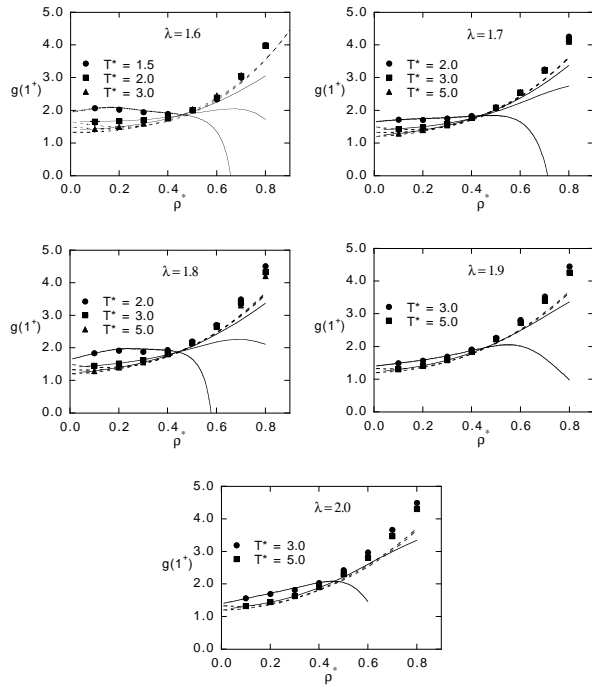


FIG. 3: Same as in Fig. 2, but for $\lambda = 1.6-2$.

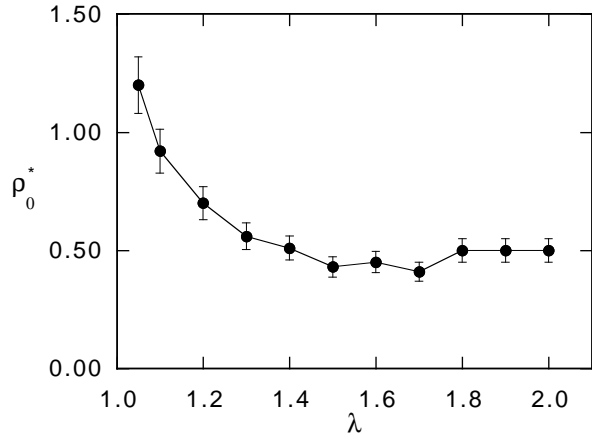


FIG. 4: Plot of the threshold density $\rho_0^*(\lambda)$ as a function of the potential range λ . For each value of λ , ρ_0^* is defined as the density around which the MC contact values $g(1^+)$ are practically insensitive to the temperature. Below (above) the curve, the YS (TL) theory can be considered as reliable. The line is a guide to the eye.

model. A second reason has to do with the construction of the YS model as an extension of Baxter's solution of the PY integral equation for sticky hard spheres, so that in principle it is intended to be a model for narrow wells.

A plot of $\rho_0^*(\lambda)$ is presented in Fig. 4. It can be interpreted as a sort of “phase” diagram in which the curve separates the respective regions where the TL and YS theories are reliable for moderate temperatures in the interval $T_c^*(\lambda) \lesssim T^* \lesssim 3T_c^*(\lambda)$. We observe that as the range λ decreases, the YS region tends to span the whole

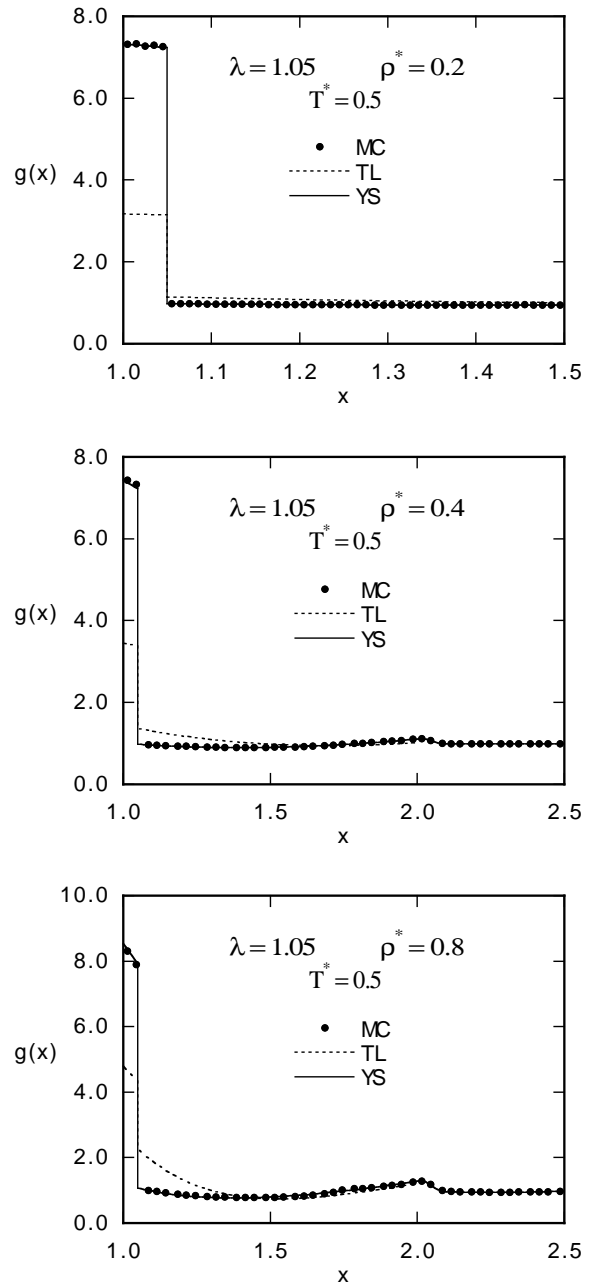


FIG. 5: Comparison of the r.d.f. obtained from the TL (dotted lines) and YS (solid lines) theories with Monte Carlo data (circles) for $\lambda = 1.05$ and $T^* = 0.5$. Note that the TL curves are interrupted after $x = 2$.

fluid density domain. In addition, ρ_0^* presents a minimum $\rho_0^* \approx 0.4$ at $\lambda \approx 1.7$, so the YS theory does a fairly good job if $\rho^* \lesssim 0.4$, even for wide potentials.

Once we have analyzed the performances of the TL and YS theories in connection with the contact value $g(1^+)$, let us proceed to investigate the r.d.f. $g(x)$ itself. The results are presented in Figs. 5–10. Since in this paper we are mainly interested in short-ranged SW potentials, we have paid special attention to the ranges $1.05 \leq \lambda \leq 1.3$

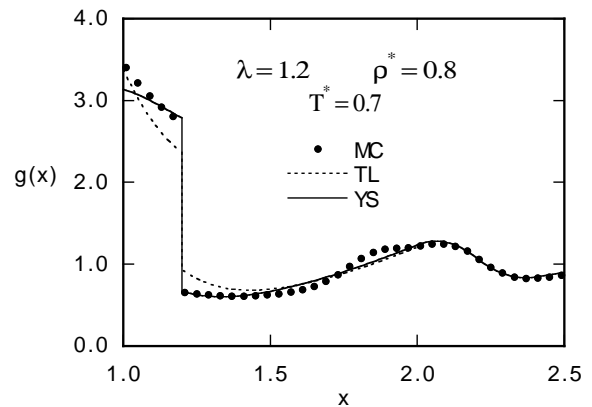
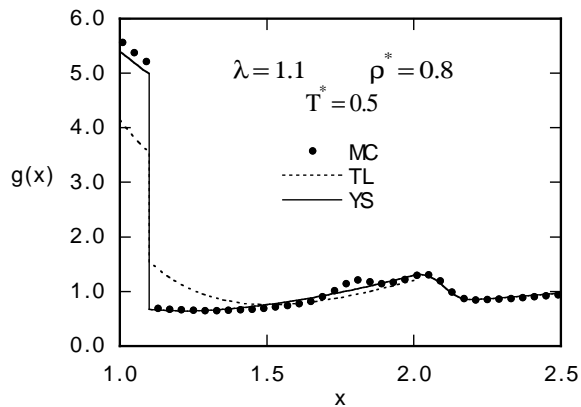
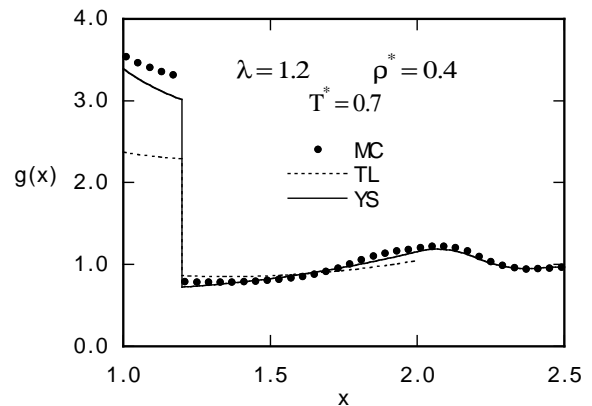
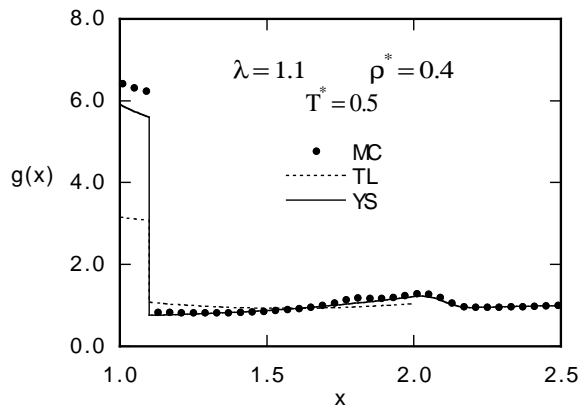
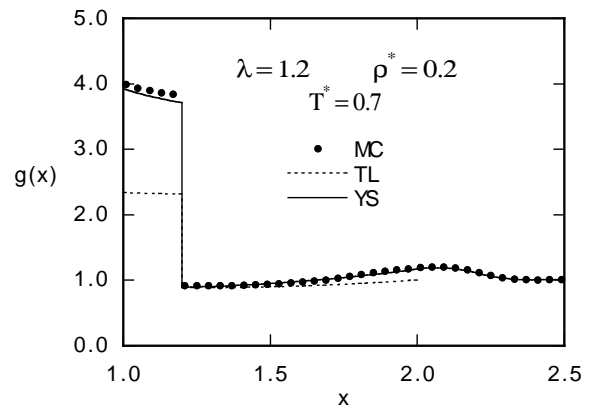
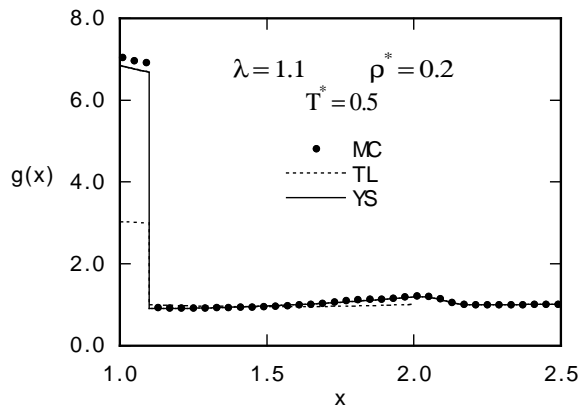


FIG. 6: Same as in Fig. 5, but for $\lambda = 1.1$ and $T^* = 0.5$.

FIG. 7: Same as in Fig. 5, but for $\lambda = 1.2$ and $T^* = 0.7$.

(Figs. 5–8). As representative examples of a moderate and of a wide range we have considered $\lambda = 1.5$ (Fig. 9) and $\lambda = 2.0$ (Fig. 10), respectively. For each value of λ we have restricted ourselves to the lowest temperature represented in Fig. 1 and to the densities $\rho^* = 0.2, 0.4$, and 0.8 (except in the case $\lambda = 2.0$, where $\rho^* = 0.8$ has not been considered because the YS model fails to have a solution in that case). In agreement with the analysis of Figs. 2 and 3, one can see that the YS theory works well for small potential widths ($\lambda \leq 1.2$) for the whole density range. For larger potential widths, the performance of the theory is still fair at low ($\rho^* = 0.2$) and even moderate

($\rho^* = 0.4$) densities. However, the YS theory fails, and even can become entirely unphysical, at high densities ($\rho^* = 0.8 > \rho_0^*$). Of course, at temperatures higher than those of Figs. 5–10 the performance of the theory at high densities improves (not shown).

By contrast, the TL theory presents the opposite behavior to that of the YS theory, since its accuracy increases as the density and the potential width grow. Of course, it also improves if the temperature increases, as expected from a perturbation theory. According to Figs. 5–10, the TL theory does a better job than the YS model at $\rho^* = 0.8$ for $\lambda \geq 1.3$, in agreement with the “phase”

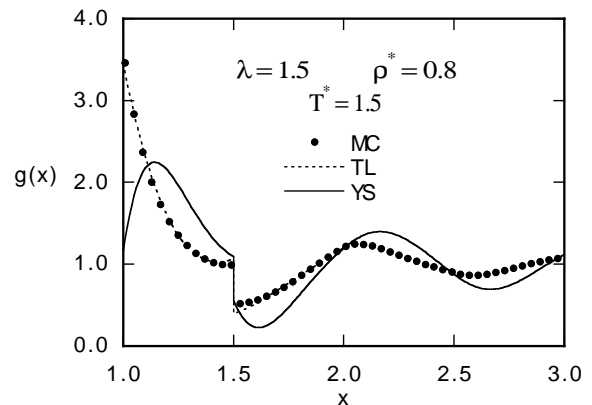
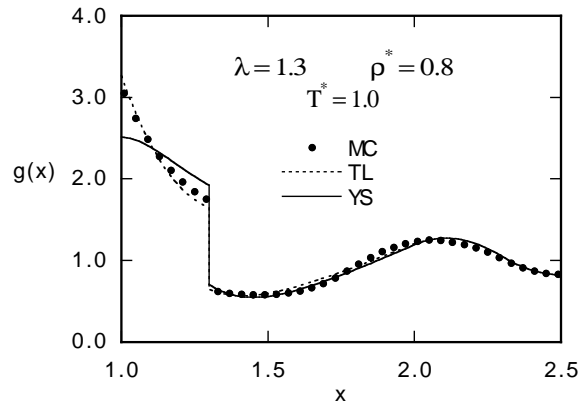
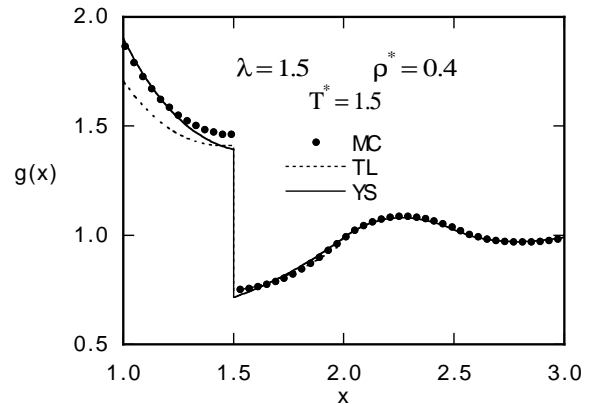
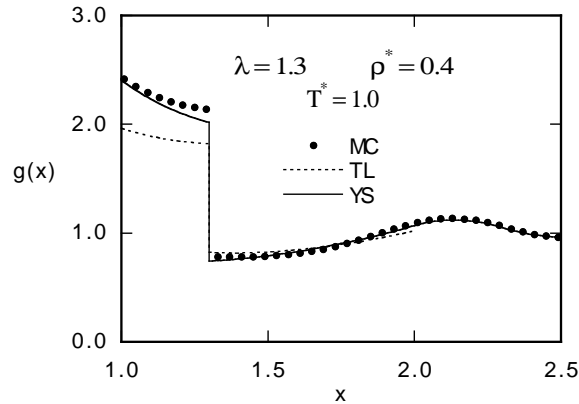
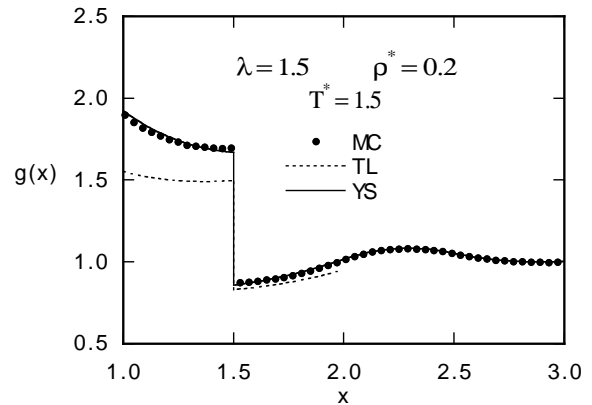
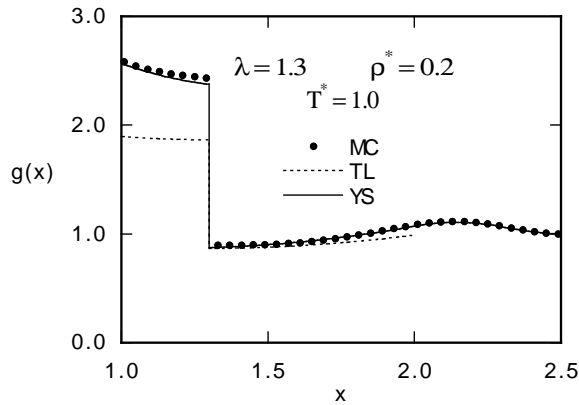


FIG. 8: Same as in Fig. 5, but for $\lambda = 1.3$ and $T^* = 1.0$.

FIG. 9: Same as in Fig. 5, but for $\lambda = 1.5$ and $T^* = 1.5$.

diagram of Fig. 4.

V. CONCLUSIONS

In this paper we have presented extensive Monte Carlo simulations for the structural properties of square-well fluids with ranges λ , reduced densities ρ^* , and reduced temperatures T^* in the intervals $1.05 \leq \lambda \leq 2$, $0.1 \leq \rho^* \leq 0.8$ and $T_c^*(\lambda) \lesssim T^* \lesssim 3T_c^*(\lambda)$, respectively. The MC data have been used to assess the accuracy of two theories that provide explicit expressions of the r.d.f. in

Laplace space, the TL perturbation theory^{27,28} and the non-perturbative YS model.²⁹

The results show that both theories complement each other, as the YS theory works well where the TL theory fails and vice versa. More specifically, the YS theory exhibits a good agreement with the MC data at any fluid density if the potential well is sufficiently narrow (say $\lambda \leq 1.2$), as well as for any width if the density is small enough (say $\rho^* \leq 0.4$). This can be further refined by noticing that the YS theory works well if $\rho^* \lesssim \rho_0^*(\lambda)$, where $\rho_0^*(\lambda)$ is the density around which the simulation data for the contact value $g(1^+)$ show the least influence

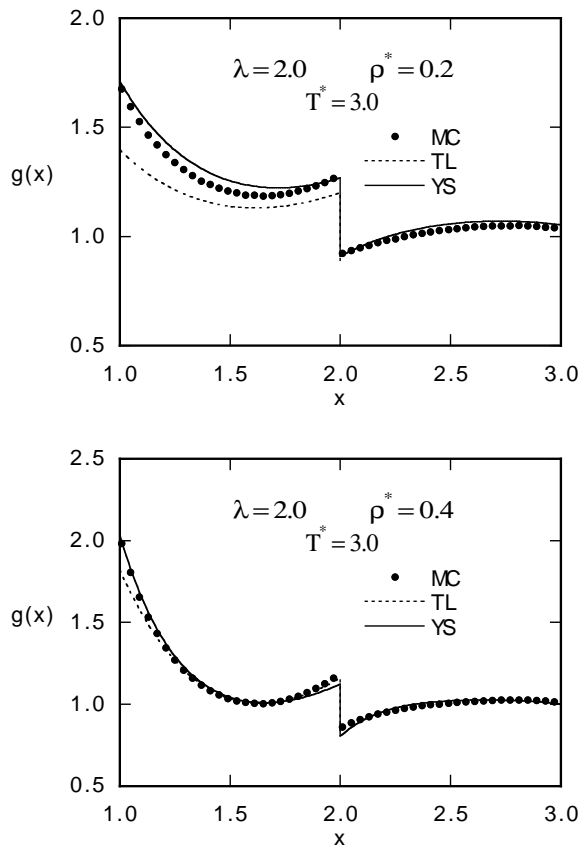


FIG. 10: Same as in Fig. 5, but for $\lambda = 2.0$ and $T^* = 3.0$.

on temperature. On the other hand, for $\rho^* > \rho_0^*(\lambda)$ the YS theory rapidly deteriorates, especially for temperatures near the critical one, while the TL theory becomes very accurate.

The complementarity between the TL and YS theories is interesting because they present some formal similarities in their formulation and are (practically) equally easy to implement (see Appendices A and B). The latter theory, however, has some advantages over the former one. First, the YS theory is especially useful for describing colloidal dispersions modeled as short-ranged SW fluids. Second, it provides a simple analytical expression for the second shell ($2 \leq x \leq 3$) of the r.d.f., whereas this is not the case for the TL theory.²⁸ Last, it seems feasible to improve the performance of the YS theory at high densities by imposing additional constraints to the Laplace transform of the r.d.f. to determine the parameter A in Eq. (4) as a function of density. Instead, in order to improve the TL theory it would be necessary to obtain higher order terms in the expansion of the r.d.f. of the SW fluid in power series of the inverse of the reduced temperature T^* , and this seems to be too complicated at present.

Acknowledgments

The present work has been partially supported by the Spanish Dirección General de Investigación (DGI) under grants No. BFM2003-001903 (J.L. and J.R.S) and No. FIS2004-01399 (S.B.Y. and A.S.).

APPENDIX A: EXPLICIT EXPRESSIONS IN THE TANG-LU THEORY

Let us define the Laplace transform $G(s)$ of $xg(x)$:

$$G(t) = \int_1^\infty dx e^{-tx} xg(x). \quad (\text{A1})$$

The contact value $g(1^+)$ is given from $G(s)$ as

$$g(1^+) = \lim_{t \rightarrow \infty} te^t G(t). \quad (\text{A2})$$

The exact solution of the PY equation for hard spheres^{54,55} reads

$$G_0(t) = t \frac{L(t)e^{-t}}{S(t) + 12\eta L(t)e^{-t}}, \quad (\text{A3})$$

where $\eta = \frac{\pi}{6}\rho\sigma^3$ is the packing fraction and

$$L(t) = 1 + 2\eta + (1 + \eta/2)t, \quad (\text{A4})$$

$$S(t) = -12\eta(1 + 2\eta) + 18\eta^2 t + 6\eta(1 - \eta)t^2 + (1 - \eta)^2 t^3. \quad (\text{A5})$$

The corresponding contact value is

$$g_0(1^+) = \frac{1 + \eta/2}{(1 - \eta)^2}. \quad (\text{A6})$$

Equation (A3) provides the zeroth-order term in the TL perturbation theory. The first-order term is^{27,28}

$$G_1(t) = -\frac{(1 - \eta)^4 e^{-t}}{Q_0^2(t)} \left\{ \frac{t^4(1 + \lambda t)}{S^2(-t)} e^{-(\lambda-1)t} - \sum_{i=1}^3 \frac{t_i^3}{(t + t_i)S_1^2(t_i)} \left[\frac{t_i(1 - \lambda t_i)}{t + t_i} + t_i(1 - \lambda t_i) \right] \times \frac{S_2(t_i)}{S_1(t_i)} - 4 + (1 + 4\lambda)t_i + \lambda(\lambda - 1)t_i^2 \right\} \times e^{(\lambda-1)t_i}, \quad (\text{A7})$$

where $S_1(t) \equiv S'(t)$, $S_2(t) \equiv S''(t)$, the primes denoting derivatives with respect to t , and

$$Q_0(t) \equiv \frac{S(t) + 12\eta L(t)e^{-t}}{(1 - \eta)^2 t^3}. \quad (\text{A8})$$

In Eq. (A7) the summation extends over the three zeroes of $S(t)$, denoted by t_i . The contact value $g_1(1^+)$ is

$$g_1(1^+) = (1 - \eta)^4 \sum_{i=1}^3 \frac{t_i^3}{S_1^2(t_i)} \left[t_i(1 - \lambda t_i) \frac{S_2(t_i)}{S_1(t_i)} - 4 \right. \\ \left. + (1 + 4\lambda)t_i + \lambda(\lambda - 1)t_i^2 \right] e^{(\lambda-1)t_i} \quad (\text{A9})$$

By analytical inversion of $G_1(t)$ one can get explicit expressions for $g_1(x)$ inside the shells $n \leq x \leq n + 1$, which become increasingly more complicated as n grows. The expression for the first shell $1 \leq x \leq 2$ can be found in Ref. 28.

APPENDIX B: EXPLICIT EXPRESSIONS IN THE YUSTE-SANTOS MODEL

By imposing the exact condition $G(t) - t^{-2} \sim t$ for small t , where $G(t)$ is defined by Eq. (A1), one can express the parameters K_1 , S_1 , S_2 , and S_3 appearing in Eq. (4) as linear functions of A and K_2 .^{29,30}

$$K_1 = \frac{1}{1 + 2\eta} \left[1 + \frac{\eta}{2} + 2\eta(\lambda^3 - 1)K_2 \right. \\ \left. - \frac{\eta}{2}(\lambda^4 - 4\lambda + 3)A \right] + K_2 - A(\lambda - 1), \quad (\text{B1})$$

$$S_1 = \frac{\eta}{1 + 2\eta} \left[-\frac{3}{2} + 2(\lambda^3 - 1)K_2 - \frac{1}{2}(\lambda^4 - 4\lambda + 3)A \right], \quad (\text{B2})$$

$$S_2 = \frac{1}{2(1 + 2\eta)} \left\{ -1 + \eta + 2[\lambda - 1 - 2\eta\lambda(\lambda^2 - 1)]K_2 \right. \\ \left. - [(\lambda - 1)^2 - \eta(\lambda^2 - 1)^2]A \right\}, \quad (\text{B3})$$

$$S_3 = \frac{1}{1 + 2\eta} \left\{ -\frac{(1 - \eta)^2}{12\eta} - \left[\frac{1}{2}(\lambda^2 - 1) - \eta\lambda^2(\lambda - 1) \right]K_2 \right. \\ \left. + \frac{1}{12}[4 + 2\lambda - \eta(3\lambda^2 + 2\lambda + 1)](\lambda - 1)^2A \right\}. \quad (\text{B4})$$

From Eq. (A2), we have

$$g(1^+) = \frac{K_1}{12\eta S_3}. \quad (\text{B5})$$

By application of the Heaviside expansion theorem, the inverse Laplace transform of $tF(t)$ reads

$$f_1(x) = f_{10}(x)\Theta(x) + f_{11}(x + 1 - \lambda)\Theta(x + 1 - \lambda), \quad (\text{B6})$$

where

$$f_{1k}(x) = -\frac{1}{12\eta} \sum_{i=1}^3 \frac{C_{1k}(t_i)}{S'(t_i)} t_i e^{t_i x}. \quad (\text{B7})$$

Here, t_i are the three distinct roots of $S(t) \equiv 1 + S_1 t + S_2 t^2 + S_3 t^3$ [not to be confused with the polynomial (A5)] and

$$C_{10}(t) \equiv 1 + A + K_1 t, \quad C_{11}(t) \equiv -(A + K_2 t). \quad (\text{B8})$$

Analogously, the inverse Laplace transform of $t[F(t)]^2$ is

$$f_2(x) = f_{20}(x)\Theta(x) + f_{21}(x + 1 - \lambda)\Theta(x + 1 - \lambda) \\ + f_{22}(x + 2 - 2\lambda)\Theta(x + 2 - 2\lambda), \quad (\text{B9})$$

where

$$f_{2k}(x) = \frac{1}{(12\eta)^2} \sum_{i=1}^3 \left[x C_{2k}(t_i) + C'_{2k}(t_i) \right. \\ \left. - C_{2k}(t_i) \frac{S''(t_i)}{S'(t_i)} \right] \frac{e^{t_i x}}{[S'(t_i)]^2}, \quad (\text{B10})$$

where we have called

$$C_{20}(t) \equiv t[C_{10}(t)]^2, \quad C_{21}(t) \equiv 2tC_{10}(t)C_{11}(t), \\ C_{22}(t) \equiv t[C_{11}(t)]^2. \quad (\text{B11})$$

Insertion of Eqs. (B6) and (B9) into Eq. (5) gives the r.d.f. $g(x)$ in the interval $1 \leq x \leq 3$. Note that the contribution $f_{22}(x)$ is needed inside that interval only if $\lambda < \frac{3}{2}$. For $x > 3$ the evaluation of $f_3(x), f_4(x), \dots$ is required. Alternatively, one can make use of the efficient method discussed by Abate and Whitt⁶⁰ to invert numerically Laplace transforms.

To close the model, we need to determine the parameters A and K_2 . The former is assigned its zero-density limit value, namely $A = e^{1/T^*} - 1$.²⁹ To determine K_2 we impose the continuity condition of the cavity function at $x = \lambda$, what implies

$$g(\lambda^-) = e^{1/T^*} g(\lambda^-). \quad (\text{B12})$$

This yields

$$\left(1 - e^{-1/T^*} \right) f_{10}(\lambda - 1) = -f_{11}(0) = -\frac{K_2}{12\eta S_3}. \quad (\text{B13})$$

Since the roots t_i depend on K_2 through the coefficients S_1, S_2 , and S_3 , Eq. (B13) is a transcendental equation for K_2 that needs to be solved numerically. Acedo and Santos have recently proposed a simplified version of the YS model whereby the exact condition (B12) is replaced by a simpler one that allows K_2 to be obtained analytically.³⁰ This is especially useful for determining the thermodynamic properties.^{10,30} In this paper, however, since we are interested in the structural properties, we enforce condition (B12) and determine K_2 from Eq. (B13).

- * largoju@unican.es
 † solanajr@unican.es; Author to whom correspondence should be addressed
 ‡ santos@unex.es; <http://www.unex.es/fisteor/santos/sby>
 § andres@unex.es; <http://www.unex.es/fisteor/andres/>
- ¹ J. A. Barker and D. Henderson., *J. Chem. Phys.* **47**, 2856 (1967).
 - ² W. R. Smith, D. Henderson, and J. A. Barker, *J. Chem. Phys.* **53**, 508 (1970).
 - ³ W. R. Smith, D. Henderson, and J. A. Barker, *J. Chem. Phys.* **55**, 4027 (1971).
 - ⁴ D. Henderson, J. A. Barker, and W. R. Smith, *J. Chem. Phys.* **64**, 4244 (1976).
 - ⁵ D. Henderson, O. H. Scalise, and W. R. Smith, *J. Chem. Phys.* **72**, 2431 (1980).
 - ⁶ J. A. Barker and D. Henderson, *Rev. Mod. Phys.* **48**, 587 (1976).
 - ⁷ J. Chang and S. I. Sandler, *Mol. Phys.* **81**, 745 (1994).
 - ⁸ A. L. Benavides and A. Gil-Villegas, *Mol. Phys.* **97**, 1225 (1999).
 - ⁹ J. Largo and J. R. Solana, *Molecular Simulation* **29**, 363 (2003).
 - ¹⁰ J. Largo, J. R. Solana, L. Acedo, and A. Santos, *Mol. Phys.*, **101**, 2981 (2003).
 - ¹¹ Y. Tago, *J. Chem. Phys.* **58**, 2096 (1973).
 - ¹² Y. Tago, *Phys. Lett. A* **44**, 43 (1973).
 - ¹³ Y. Tago, *J. Chem. Phys.* **60**, 1528 (1974).
 - ¹⁴ D. Henderson, W. G. Madden, and D. D. Fitts, *J. Chem. Phys.* **64**, 5026 (1976).
 - ¹⁵ W. R. Smith, D. Henderson, and Y. Tago, *J. Chem. Phys.* **67**, 5308 (1977).
 - ¹⁶ W. R. Smith and D. Henderson, *J. Chem. Phys.* **69**, 319 (1978).
 - ¹⁷ G. L. Jones, J. J. Kozak, E. Lee, S. Fishman, and M. E. Fisher, *Phys. Rev. Lett.* **46**, 795 (1981).
 - ¹⁸ G. Kahl and J. Hafner, *Phys. Chem. Liq.* **12**, 109 (1982), and references therein.
 - ¹⁹ G. Sarkisov, D. Tikhonov, J. Malinsky, and Y. Magarshak, *J. Chem. Phys.* **99**, 3926 (1993).
 - ²⁰ A. Gil-Villegas, C. Vega, F. del Río, and A. Malijevský, *Mol. Phys.* **86**, 857 (1995).
 - ²¹ J. Bergenholtz, P. Wu, N. J. Wagner, and B. D'Aguaño, *Mol. Phys.* **87**, 331 (1996).
 - ²² C. Caccamo, *Phys. Rep.* **274**, 1 (1996), and references therein.
 - ²³ A. Lang, G. Kahl, C. N. Likos, H. Löwen, and M. Watzlawek, *J. Phys.: Condens. Matter* **11**, 10143 (1999), and references therein.
 - ²⁴ A. Reiner and G. Kahl, *J. Chem. Phys.* **117**, 4925 (2002).
 - ²⁵ I. Nezbeda, *Czech. J. Phys. B* **27**, 247 (1977).
 - ²⁶ R. V. Sharma and K. C. Sharma, *Physica A* **89**, 213 (1977).
 - ²⁷ Y. Tang and B. C.-Y. Lu, *J. Chem. Phys.* **100**, 3079 (1994).
 - ²⁸ Y. Tang and B. C.-Y. Lu, *J. Chem. Phys.* **100**, 6665 (1994).
 - ²⁹ S. B. Yuste and A. Santos, *J. Chem. Phys.* **101**, 2355 (1994).
 - ³⁰ L. Acedo and A. Santos, *J. Chem. Phys.* **115**, 2805 (2001).
 - ³¹ A. Rotenberg, *J. Chem. Phys.* **43**, 1198 (1965).
 - ³² B. J. Alder, D. A. Young, and M. A. Mark, *J. Chem. Phys.* **56**, 3013 (1971).
 - ³³ Y. Rosenfeld and R. Thienberger, *J. Chem. Phys.* **63**, 1875 (1975).
 - ³⁴ D. A. Young and B. J. Alder, *J. Chem. Phys.* **73**, 2430 (1980).
 - ³⁵ G. A. Chapela and S. E. Martínez-Casas, *J. Chem. Phys.* **86**, 5683 (1987).
 - ³⁶ D. A. de Lonngi, P. A. Longgi, and J. Alejandre, *Mol. Phys.* **71**, 427 (1990).
 - ³⁷ A. L. Benavides, J. Alejandre, and F. del Río, *Mol. Phys.* **74**, 321 (1991).
 - ³⁸ D. M. Heyes and P. J. Aston, *J. Chem. Phys.* **97**, 5738 (1992).
 - ³⁹ L. Vega, E. de Miguel, L. F. Rull, G. Jackson, and I. A. McLure, *J. Chem. Phys.* **96**, 2296 (1992).
 - ⁴⁰ E. de Miguel, *Phys. Rev. E* **55**, 1347 (1997).
 - ⁴¹ N. V. Brilliantov and J. P. Valleau, *J. Chem. Phys.* **108**, 1115 (1998).
 - ⁴² G. Orkoulas and A. Z. Panagiotopoulos, *J. Chem. Phys.* **110**, 1581 (1999).
 - ⁴³ J. R. Elliott and L. Hu, *J. Chem. Phys.* **110**, 3043 (1999).
 - ⁴⁴ G. Orkoulas, M. E. Fisher, and A. Z. Panagiotopoulos, *Phys. Rev. E* **63**, 051507 (2001).
 - ⁴⁵ S. Labík, A. Malijevský, R. Kao, W. R. Smith, and F. del Río, *Mol. Phys.* **96**, 849 (1999).
 - ⁴⁶ F. del Río, E. Ávalos, R. Espíndola, L. F. Rull, G. Jackson, and S. Lago, *Mol. Phys.* **100**, 2531 (2002).
 - ⁴⁷ J. K. Singh, D. A. Kofke, and J. R. Errington, *J. Chem. Phys.* **119**, 3405 (2003).
 - ⁴⁸ J. Largo and J. R. Solana, *Phys. Rev. E* **67**, 066112 (2003). See also the electronic publication of the American Physical Society (epaps) E-PLIEEE8-67-132306 which may be downloaded via ftp at the URL ftp://ftp.aip.org/epaps/phys_rev_e/.
 - ⁴⁹ J. S. Huang, S. A. Safran, M. W. Kim, G. S. Grest, M. Kotlarchyk, and N. Quirke, *Phys. Rev. Lett.* **53**, 592 (1984).
 - ⁵⁰ E. Zaccarelli, G. Foffi, K. A. Dawson, F. Sciortino, and P. Tartaglia, *Phys. Rev. E* **63**, 031501 (2001).
 - ⁵¹ K. Dawson, G. Foffi, M. Fuchs, W. Götze, F. Sciortino, M. Sperl, P. Tartaglia, Th. Voigtmann, and E. Zaccarelli, *Phys. Rev. E* **63**, 011401 (2001).
 - ⁵² E. Zaccarelli, G. Foffi, K. A. Dawson, S. V. Buldyrev, F. Sciortino, and P. Tartaglia, *J. Phys.: Condens. Matter* **15**, S367 (2003).
 - ⁵³ A. Lomakin, N. Asherie, and G. B. Bendek, *J. Chem. Phys.* **104**, 1646 (1996).
 - ⁵⁴ M. S. Wertheim, *Phys. Rev. Lett.* **10**, 321 (1963).
 - ⁵⁵ E. Thiele, *J. Chem. Phys.* **39**, 474 (1963).
 - ⁵⁶ J. Largo and J. R. Solana, *Fluid Phase Equilibria* **212**, 11 (2003).
 - ⁵⁷ K. Shukla and R. Rajagopalan, *Mol. Phys.* **81**, 1093 (1994).
 - ⁵⁸ R. J. Baxter, *J. Chem. Phys.* **49**, 2770 (1968).
 - ⁵⁹ One can check that the simulation values of the ratio $g(\lambda^-)/g(\lambda^+)$ deviate from the exact relationship $g(\lambda^-)/g(\lambda^+) = e^{1/T^*}$ less than 0.6% in all the cases and less than 0.2% in most of the cases.
 - ⁶⁰ J. Abate and W. Whitt, *Queueing Systems* **10**, 5 (1992).